Growth Dynamics of the Convectively Mixed Layer

L. MAHRT[1] AND D. H. LENSCHOW

National Center for Atmospheric Research,[2] Boulder, Colo. 80303

(Manuscript received 25 June 1975, in revised form 2 September 1975)

ABSTRACT

A model for the growth of a convectively mixed layer is derived by layer integrating the basic equations and parameterizing unknown terms in the mixed layer turbulence kinetic energy equation by means of free convection similarity theory. When shear generation of turbulence energy is neglected in the turbulent inversion layer capping the mixed layer, the model essentially reduces to that of Tennekes. This shear generation is found to be important only in cases of significant baroclinicity and shallow mixed layer depth or small free flow stratification.

1. Introduction

The mixed layer growing within a stably stratified fluid is capped by a thin layer of anomalously strong stratification. In the atmosphere, this thin layer is referred to as the inversion or potential temperature jump. Growth of the mixed layer and lifting of the inversion results from entrainment of air of higher potential temperature from the overlying free flow into the mixed layer. The entrainment rate is restricted since downward heat flux corresponds to the conversion of turbulence kinetic energy to potential energy. Thus, the mixed layer can entrain air from above the inversion only at a rate that is determined in part by the generation of turbulence kinetic energy in the mixed layer. To include such entrainment effects, Lilly (1968), Tennekes (1973), Niiler (1975) and others employ simple versions of the turbulence energy equation. Nonstationarity of the turbulence energy budget at the top of the mixed layer is explicitly included by Zilitinkevich (1975). Such models appear to be reasonably successful at predicting mixed layer growth yet retain appealing simplicity. For a more detailed look at the evolution of theory for mixed-layer growth, the reader is also referred to Kraus and Turner (1967), Carson (1973), Denman (1973), Pollard *et al.* (1973), Stull (1973) and Thompson (1973).

The following development attempts to include influences of the turbulent portion of the inversion layer capping the convectively mixed layer [hereafter referred to as the turbulent inversion layer (see Fig. 1); to be more carefully defined layer]. We expect turbulence in this stable layer to be maintained by shear generation and turbulent transport of turbulence energy where the latter may occur predominantly through penetration of convective elements. The thickness of this layer may be $\sim 10\%$ of the thickness of the convectively mixed layer (Rayment and Readings, 1974; Deardorff, 1969, 1974a). We model this flow situation by: 1) layer integrating the basic equations across the well-mixed layer and turbulent inversion layer as suggested by Niiler (1975); 2) employing free convection similarity theory for the mixed layer; and 3) developing a relationship to estimate the thickness of the turbulent inversion layer. The employment of free convection similarity theory greatly simplifies the turbulence kinetic energy budget and at the same time appears to be a good approximation of conditions approaching free convection (Willis and Deardorff, 1974; Lenschow, 1974; Pennell and LeMone, 1974). We expect the atmospheric planetary boundary layer to generally approach such conditions whenever surface heating is appreciable such as occurs over land with mostly sunny skies (excluding conditions of low sun angle, high surface albedo, etc.), or as might occur in cold air outbreaks over warm surfaces. Free convection similarity theory is also expected to be a good approximation to the oceanic mixed layer under conditions of significant surface cooling.

An important goal of the present development is to retain simplicity to the extent that the number of free parameters can be restricted and that approximate analytical solutions can be obtained to assist in understanding the physics of the model.

2. Governing equations

If horizontal advections are neglected, the averaged equations of motion and the averaged thermodynamic,

[1] On leave from the Department of Atmospheric Sciences, Oregon State University, Corvallis.

[2] The National Center for Atmospheric Research is sponsored by the National Science Foundation.

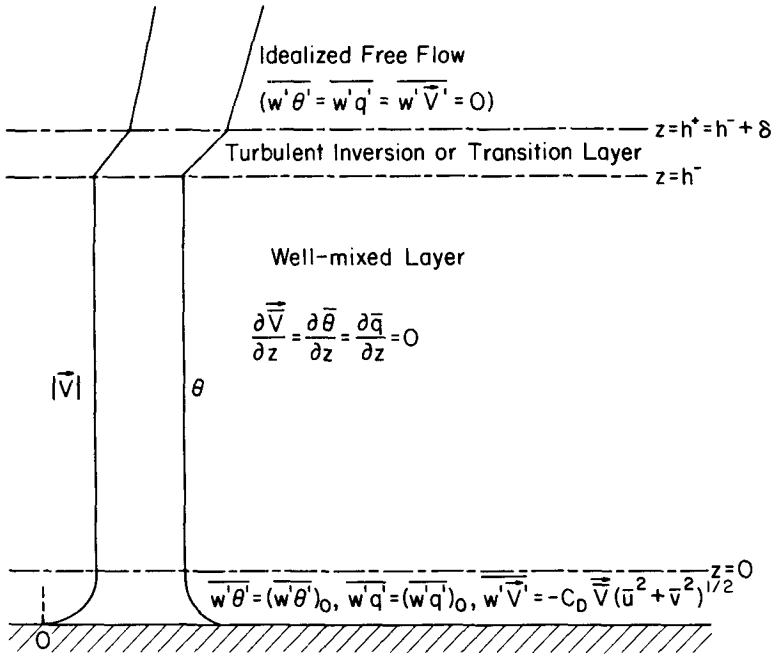

FIG. 1. Idealized planetary boundary layer.

moisture and turbulence energy equations become:

$$\frac{\partial \bar{u}}{\partial t} + \bar{w}\frac{\partial \bar{u}}{\partial z} = f\bar{v} - fV_g - \frac{\partial}{\partial z}\overline{u'w'} \tag{1}$$

$$\frac{\partial \bar{v}}{\partial t} + \bar{w}\frac{\partial \bar{v}}{\partial z} = -f\bar{u} + fU_g - \frac{\partial}{\partial z}\overline{v'w'} \tag{2}$$

$$\frac{\partial \bar{\theta}}{\partial t} + \bar{w}\frac{\partial \bar{\theta}}{\partial z} = -\frac{\partial \overline{w'\theta'}}{\partial z} + Q \tag{3}$$

$$\frac{\partial \bar{q}}{\partial t} + \bar{w}\frac{\partial \bar{q}}{\partial z} = -\frac{\partial \overline{w'q'}}{\partial z} \tag{4}$$

$$\frac{\partial \overline{E'}}{\partial t} + \bar{w}\frac{\partial \overline{E'}}{\partial z} = -\overline{w'\mathbf{V}'}\cdot\frac{\partial \bar{\mathbf{V}}}{\partial z} + \frac{g}{\theta_0}\overline{w'\theta'} - \frac{\partial}{\partial z}[\overline{w'(P'/\rho_0 + E')}] - \epsilon \tag{5}$$

where

$$\overline{E'} \equiv \tfrac{1}{2}(\overline{u'^2} + \overline{v'^2} + \overline{w'^2}),$$

θ is the virtual potential temperature, Q the radiational divergence term, q specific humidity, ϵ the dissipation rate of turbulence kinetic energy, ρ_0 and θ_0 are constant representative values, and fV_g and fU_g are the constant large-scale horizontal pressure gradient terms; the overbar denotes a time average and the other terms are defined in the usual meteorological sense. The effects of latent heat release are neglected. Vertical advection is included since it may be important in the turbulent inversion layer (where vertical gradients are large) even when horizontal advections and vertical motions are small. These equations are evaluated in the well-mixed and turbulent inversion layers while the surface layer and the free flow region above the boundary layer are parameterized as boundary conditions.

a. Well-mixed layer

We consider the following idealized mixed layer:

1) Vertical gradients of virtual potential temperature, wind and specific humidity are negligibly small. Wind shear may be small in a convectively mixed layer even with baroclinicity (Arya and Wyngaard, 1975). However, the well-mixed assumption is expected to be better for virtual potential temperature than for wind and specific humidity since thermal stratification and convective mixing are strongly coupled.

2) The turbulence virtual heat flux decreases linearly with height. This is in good agreement with observations and simulations of convectively mixed boundary layers except near the top where substantial curvature is observed (Lenschow, 1974; Willis and Deardorff, 1974; Deardorff, 1974b). Corrections for such curvature are excluded in this development.

3) The dissipation of turbulence kinetic energy is independent of height in the convectively mixed layer above the surface layer. This assumption is in good agreement with the above studies.

4) The turbulence energy in the mixed layer and turbulent inversion layer adjusts rapidly to the bulk shear and turbulent fluxes so that $d\overline{E'}/dt$ can be

neglected in the turbulence energy equation. That is, an approximate balance between remaining terms is maintained. Such an approximate balance is argued by Lilly (1968) in terms of the small dissipation time scale. In the case of zero mean vertical motion, this assumption implies that local time changes of turbulence energy within the mixed layer can be neglected. However, turbulence energy at a fixed level near the mixed layer top and the total turbulence energy of the mixed layer increase with time since

$$\frac{\partial}{\partial t}\int_0^{h^-}\overline{E'}dz=\int_0^{h^-}\frac{\partial}{\partial t}(\overline{E'})dz+(\overline{E'})_{h^-}\frac{\partial h^-}{\partial t}\approx(\overline{E'})_{h^-}\frac{\partial h^-}{\partial t}.$$

In other words, nonstationarity of the turbulence energy is assumed to be important only in the turbulent inversion layer where turbulence is "spun-up" to the quasi-equilibrium state of the mixed layer.

We now integrate (1)–(5) from a reference level near the top of the surface layer, $z=0$, to the top of the mixed layer, h^-. For this integration we use the above assumptions and apply Leibniz's rule at h^-. Stress at the bottom of the mixed layer is parameterized with a drag law, employing a drag coefficient C_D. The basic equations then become:

$$\frac{\partial\bar{u}}{\partial t}=f\bar{v}-\frac{f}{h^-}\int_0^{h^-}V_g dz-\frac{(\overline{u'w'})_{h^-}}{h^-}-\frac{C_D\bar{u}}{h^-}[\bar{u}^2+\bar{v}^2]^{\frac{1}{2}} \quad (6)$$

$$\frac{\partial\bar{v}}{\partial t}=-f\bar{u}+\frac{f}{h^-}\int_0^{h^-}U_g dz-\frac{(\overline{v'w'})_{h^-}}{h^-}-\frac{C_D\bar{v}}{h^-}[\bar{u}^2+\bar{v}^2]^{\frac{1}{2}} \quad (7)$$

$$\frac{\partial\bar{\theta}}{\partial t}=\frac{1}{h^-}[-(\overline{w'\theta'})_{h^-}+(\overline{w'\theta'})_0]+\frac{1}{h^-}\int_0^{h^-}Q dz \quad (8)$$

$$\frac{\partial\bar{q}}{\partial t}=\frac{1}{h^-}[-(\overline{w'q'})_{h^-}+(\overline{w'q'})_0] \quad (9)$$

$$0=-\left[\overline{w'\left(\frac{P'}{\rho_0}+E'\right)}\right]_{h^-}+\left[\overline{w'\left(\frac{P'}{\rho_0}+E'\right)}\right]_0 -\epsilon h^-+\frac{gh^-}{2\theta_0}[(\overline{w'\theta'})_{h^-}+(\overline{w'\theta'})_0]. \quad (10)$$

b. Turbulent inversion layer

We define δ to be the thickness of the turbulent stably stratified layer capping the mixed layer. This layer cannot always be clearly defined from observations. One reason is that the structure of the inversion capping a convectively mixed boundary layer varies substantially in time and space as observed, for example, by Rayment and Readings (1974) and Readings *et al.* (1973). The occurrence of turbulence is by no means continuous in space or time and the turbulence may involve the breaking of Kelvin-Helmholtz type waves. The occurrence of such turbulence in low-level, stably stratified layers has been examined in some detail in a number of recent studies, including Kerman (1974) and Metcalf and Atlas (1973).

In the present idealized model we do not explicitly consider horizontal inhomogeneities in inversion height and structure. We also do not consider temporal variations of the inversion structure on the time scales of gravity or Kelvin-Helmholtz type waves or undulations in the inversion induced by convective elements. We consider δ to be representative of a typical instantaneous thickness as opposed to the thickness of the layer within which the inversion layer undulates. We thus model increases in the inversion height on the diurnal time scale.

We make the following additional assumptions about the turbulent inversion layer and overlying free atmosphere:

1) To integrate the turbulence kinetic energy equation, we assume that velocities, fluxes and dissipation of turbulence kinetic energy decrease linearly with height across the thin turbulent inversion layer.

2) The turbulent inversion layer is sufficiently thin so that terms of $O(\delta)$ can be neglected in the integrated equations. An analogous assumption is employed by Niiler (1975). Since we will be adding these equations to their corresponding mixed layer equations, this assumption is analogous to assuming $\delta/h_{-}\ll 1$.

3) Diabatic heating and fluxes due to turbulence and wave motions are neglected in the idealized free atmosphere. This assumption precludes, for example, active cumulus clouds immediately above the mixed layer where latent heating and turbulent exchanges with the mixed layer may be important.

We integrate (1)–(4) across the turbulent inversion layer by using Leibniz's rule. After neglecting terms of $O(\delta)$, only terms involving vertical gradients or time dependencies remain. Noting that $\bar{\phi}_{ih^-}=\phi_i$, we obtain

$$(\overline{w'\phi_i'})_{h^-}\approx-\left[\frac{\partial h^-}{\partial t}-\bar{w}_h\right][\bar{\phi}_{ih^+}-\bar{\phi}_i]\equiv-w_e\Delta\phi_i, \quad (11)$$

where $\phi_i=(u,v,\theta,q)$, w_e is the entrainment velocity, and $\Delta\phi$ the difference in ϕ_i across the turbulent inversion layer. The procedure whereby terms of $O(\delta)$ are neglected cannot be applied to the integrated turbulence kinetic energy equation since the exact dependence of various terms on the thickness δ cannot be determined *a priori*. That is, terms in the turbulence kinetic energy equation influence the thickness δ in a complicated way. For example, the integrated buoyancy destruction term, $(\delta/2)(g/\theta_0)(\overline{w'\theta'})_{h^-}$, is not necessarily of $O(\delta)$ since we expect δ and $(\overline{w'\theta'})_{h^-}$ to be related. Even those terms in this equation that are apparently small may be important, since the net production of turbulence energy in the underlying mixed layer is a small difference

between larger terms. Thus we retain all of the terms in the integrated turbulence kinetic energy equation, in which case

$$\int_{h^-}^{h^+}\frac{d}{dt}(\overline{E'})dz=\left[\overline{w'\left(\frac{P'}{\rho_0}+E'\right)}\right]_{h^-}-\frac{(\overline{u'w'})_{h^-}-\Delta u}{2}$$
$$-\frac{(\overline{v'w'})_{h^-}-\Delta v}{2}-\epsilon_{h^-}\frac{\delta}{2}+(\overline{w'\theta'})_{h^-}\frac{\delta g}{2\theta_0}. \quad (12)$$

To reduce the number of unknowns, we add the equations for the mixed layer [(6)–(10)] to the corresponding turbulent inversion layer equations [(11), (12)]. The resulting total thermodynamic equation is subtracted from the free flow thermodynamic equation

$$\left(\frac{\partial\theta}{\partial t}\right)_{h^+}=\left(\frac{\partial h^+}{\partial t}-w_{h^+}\right)\left(\frac{\partial\theta}{\partial z}\right)_{h^+}. \quad (13)$$

The resulting set of equations is:

$$\frac{\partial\bar{u}}{\partial t}=f\bar{v}-\frac{f}{h^-}\int_0^{h^-}V_g dz+\frac{w_e}{h^-}\Delta u-\frac{C_D\bar{u}}{h^-}[\bar{u}^2+\bar{v}^2]^{\frac{1}{2}} \quad (14)$$

$$\frac{\partial\bar{v}}{\partial t}=-f\bar{u}+\frac{f}{h^-}\int_0^{h^-}U_g dz+\frac{w_e}{h^-}\Delta v-\frac{C_D\bar{v}}{h^-}[\bar{u}^2+\bar{v}^2]^{\frac{1}{2}} \quad (15)$$

$$\frac{\partial(\Delta\theta)}{\partial t}=w_e\gamma-\frac{1}{h^-}\left[w_e\Delta\theta+(\overline{w'\theta'})_0+\int_0^{h^-}Qdz\right] \quad (16)$$

$$\int_{h^-}^{h^+}\frac{d}{dt}(\overline{E'})dz$$
$$=\left[\overline{w'\left(\frac{P'}{\rho_0}+E'\right)}\right]_0-\epsilon h^-\left(1+\frac{\delta}{2h^-}\right)$$
$$+\frac{gh^-}{2\theta_0}\left[-w_e\Delta\theta\left(1+\frac{\delta}{h^-}\right)+(\overline{w'\theta'})_0\right]$$
$$+\frac{w_e}{2}[(\Delta u)^2+(\Delta v)^2] \quad (17)$$

$$\frac{\partial(\Delta q)}{\partial t}=w_e\gamma_q-\frac{1}{h^-}[w_e\Delta q+(\overline{w'q'})_0]. \quad (18)$$

Here

$$\gamma\equiv\left(\frac{\partial\theta}{\partial z}\right)_{h^+},\quad \gamma_q\equiv\left(\frac{\partial q}{\partial z}\right)_{h^+}.$$

We do not neglect terms in the turbulence energy budget of relative magnitude δ/h^- since remaining terms partially cancel each other and may sum to be comparably small. That is, only a small fraction of the turbulence energy generated in the mixed layer is available for mixing at the mixed layer top.

The equations describing the inversion strength and height [(16), (17)] are mainly coupled to the momentum equations through the shear generation of turbulence energy at the inversion. Eqs. (14)–(18) do not form a closed set of equations. Closure for flow conditions approaching free convection is the topic of the next section.

3. Free convection case

We close the above system of equations by parameterizing the upward flux of turbulence energy at the bottom of the mixed layer and the mixed layer dissipation of turbulence energy in terms of the convective velocity scale

$$w_*\equiv[(g/\theta_0)(\overline{w'\theta'})_0h^-]^{\frac{1}{3}}.$$

Guided by observations of Lenschow (1974) and laboratory measurements of Willis and Deardorff (1974), we adopt the following parameterization for the dissipation term:

$$\epsilon h^-=C_\epsilon w_*^3,\quad C_\epsilon\approx 0.4. \quad (19)$$

This form is also suggested by the scaling arguments

$$\epsilon\sim(\overline{E'})^{\frac{3}{2}}/l,\quad \overline{E'}\sim w_*^2,\quad l\sim h^-.$$

For unstable stratification, Wyngaard and Coté (1971) parameterize $(\overline{w'E'})_0$ in the form

$$(\overline{w'E'})_0=\left(\frac{z_s}{h^-}\right)w_*^3\equiv C_0w_*^3,$$

where z_s is the height above the ground of the reference level or bottom of the mixed layer $z=0$. Thus C_0 is a parameter which becomes quite small as the day proceeds.

Assuming that time changes of the turbulence energy level in a coordinate system rising with the inversion are small in the turbulent inversion layer, the term

$$\int_{h^-}^{h^+}\frac{\overline{dE'}}{dt}dz$$

can also be parameterized in terms of free convection similarity theory (Zilitinkevich, 1975), although the magnitude of a resulting dimensionless constant is at present uncertain (Tennekes, 1975). Such nonstationarity may significantly reduce the mixed layer growth rate in the morning especially during periods of rapid growth rate. Without justification, we neglect nonstationarity of turbulence energy; that is, we assume that the amount of energy needed to spin-up the entrained nonturbulent fluid to a turbulence level characteristic of the mixed layer is small compared to the amount of mechanical turbulence energy converted to potential energy via downward heat flux.

Solving for the entrainment velocity from the turbulence energy equation (17), using the above parameterizations, and neglecting the pressure transport of energy out of the surface layer, we obtain

$$\left(\frac{\partial h^-}{\partial t}-w_h\right)=\frac{\left[1+2C_0-2C_\epsilon\left(1+\frac{\delta}{2h^-}\right)\right](\overline{w'\theta'})_0}{\Delta\theta\left(1+\frac{\delta}{h^-}\right)-\frac{\theta_0}{gh^-}[(\Delta u)^2+(\Delta v)^2]}. \quad (20)$$

The numerator of (20) contains, respectively, the buoyancy generation of turbulence kinetic energy in the mixed layer, the flux of turbulence kinetic energy from the surface layer, and dissipation in the mixed layer and turbulent inversion layer. The first term in the denominator is associated with buoyancy destruction of turbulence kinetic energy in the mixed layer and turbulent inversion layer due to downward entrainment of heat. The second term is associated with the shear generation in the turbulent inversion layer. In the case of a deep mixed layer, the effects of shear generation and buoyancy destruction in the inversion layer will be small compared to the mixed layer buoyancy destruction. If the magnitude of the shear generation should approach the magnitude of the larger total buoyancy destruction, the growth rate becomes large. However, the rapid increase in mixed layer depth causes a rapid increase in the boyancy destruction which is now occurring over a deeper layer. This negative feedback mechanism will in general restrict the maximum possible growth rate.

We assume that in conditions approaching free convection, diabatic heating can be neglected compared to the comparatively large turbulence heat flux divergence. To close the system of equations [(14)–(16), (18), (20)] we must formulate an estimate of the thickness of the turbulent inversion layer.

This thickness can be estimated by using any one of the following approaches: (i) specify the bulk Richardson number for the turbulent inversion layer as suggested by Csanady (1974), (ii) assume $(\overline{w'E'})_{h^-}$ obeys free convection similarity theory, or (iii) specify a value for δ/h^-. Alternatively we could allow $\delta \to 0$ in the turbulence energy equation, but retain buoyancy destruction by specifying a Richardson number. This approach differs from the first approach in that it neglects dissipation in the turbulent inversion layer. We choose the first method which appears to be most reasonable and most general when shear generation is important. As shown in Section 4, the effect of nonzero δ for the case where shear generation is unimportant does not qualitatively affect the mixed layer growth rate.

We define R_b, a bulk Richardson number for the turbulent inversion layer, to be

$$R_b\equiv\frac{\frac{g}{\theta_0}\int_{h^-}^{h^+}\overline{w'\theta'}\,dz}{\int_{h^-}^{h^+}\left(\overline{w'\mathbf{V}'}\cdot\frac{\partial\overline{\mathbf{V}}}{\partial z}\right)dz}. \quad (21)$$

Using the flux relationship (11) and the assumption that turbulent fluxes and velocity decrease linearly with height across the turbulent inversion layer, R_b reduces to the conventional bulk Richardson number

$$R_b=\frac{g\Delta\theta\delta}{\theta_0[(\Delta u)^2+(\Delta v)^2]}. \quad (22)$$

Theoretically the critical value of this number in stably stratified turbulent air has been estimated to be roughly 0.25. Observations by Browning *et al.* (1973), Atlas *et al.* (1970) and others indicate that this value is reasonable in stably stratified regions of local turbulence genesis. However, they observed the Richardson number to vary considerably in space and time. Hall *et al.* (1975) made five measurements of the Richardson number in the turbulent inversion layer and all were less than 0.25. The estimate of this number depends directly on the uncertain estimate of the thickness of the turbulent inversion layer. Rayment and Readings (1974) and Readings *et al.* (1973) consider the inversion layer capping a convectively mixed layer to be eroded by buoyant convective elements from below, thinning the inversion layer until the Richardson number is locally reduced to its critical value. The resulting local shear-generated turbulence mixes the air with air above and below and tends to thicken the inversion layer and maintain the Richardson number close to its critical value.

Airplane measurements of the gradient Richardson number

$$\mathrm{Ri}=\frac{g\partial\bar{\theta}/\partial z}{\bar{\theta}[(\partial\bar{u}/\partial z)^2+(\partial\bar{v}/\partial z)^2]}$$

along slant flight paths through the turbulent inversion layer lend further credence to the concept of a critical Richardson number in those turbulent inversion layers where shear generation is important. Fig. 2 is an example of measurements along a traverse through the turbulent inversion layer, which appears to extend vertically from about 490 to 530 m. The airplane vertical and horizontal velocity components were about 2.3 and 79 m s^{-1}, respectively. Thus the flight path angle was about 1.7° and the airplane covered about 1.4 km horizontally while ascending through this region. The data used in this figure were interpolated from data points recorded at equal time increments to data points at equal height increments and then filtered with a

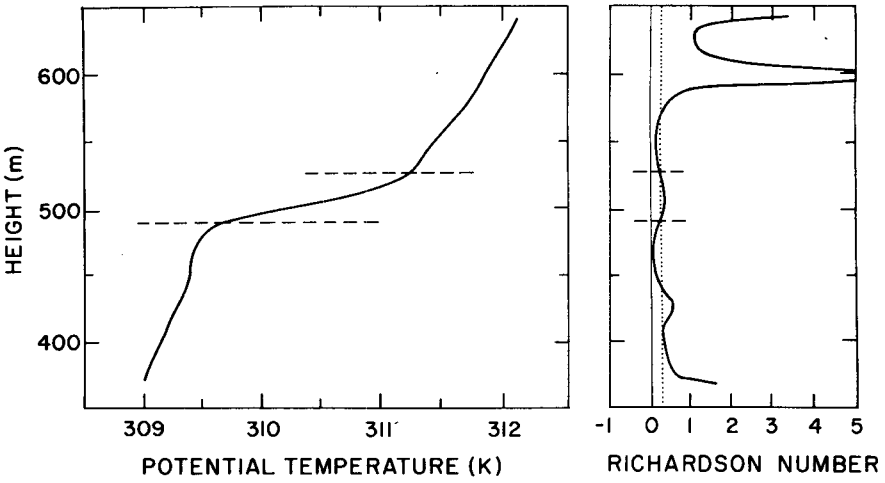

FIG. 2. Potential temperature and gradient Richardson number near the mixed layer top measured along a slant flight path by the NCAR Buffalo aircraft near Haswell, Colo., at 1000 LST 7 August 1972. Dashed lines denote possible turbulent inversion layer.

low-pass digital Gaussian filter (Holloway, 1958) with a smoothing function $\exp(-z^2/2\sigma^2)$ for $\sigma=20.26$ m (H. Isaka, unpublished manuscript). Above and below this region, the vertical gradients of temperature and velocity are too small to accurately estimate Ri because the contribution from horizontal gradients is of similar magnitude. Within the turbulent inversion layer, however, $\mathrm{Ri}\approx 0.25$ and therefore, for the layer as a whole, $\mathrm{R_b}\approx 0.25$. Although other aircraft traverses gave similar results, the close agreement with the theoretical value is probably somewhat fortuitous, since the results could be in error by as much as 50% mainly due to aliasing of the vertical gradients by the horizontal gradients of temperature and velocity.

Within the framework of (22), Niiler's model is analogous to the case $\mathrm{R_b}=0(\delta\rightarrow 0)$ while Tennekes' model does not consider shear generation. Using (22), we can specify a typical bulk Richardson for the inversion layer for the purpose of estimating δ, in which case

$$\delta=\mathrm{R_b}(\Delta\mathbf{V})^2\frac{\theta_0}{g\Delta\theta}. \tag{23}$$

However, under conditions where nonzero δ is maintained mainly by upward turbulent transport of turbulence energy, (23) is not useful, since $\delta\rightarrow 0$ as $\mathrm{R_b}\rightarrow 0$. The case of vanishing shear generation is considered in Section 4.

In Section 5, we consider some simple solutions for the case where shear generation is sufficiently important so that the bulk Richardson number criteria (23) can be used.

4. Tennekes' model

For the moment we neglect shear generation at the inversion, in which case the total turbulent energy equation (20) simplifies to

$$\left.\begin{aligned}(\overline{w'\theta'})_{h^-}&=-m(\overline{w'\theta'})_0\\ m&\equiv\left[1+2C_0-2C_\epsilon\left(1+\frac{\delta}{2h^-}\right)\right]\left(1+\frac{\delta}{h^-}\right)^{-1}\end{aligned}\right\}. \tag{24}$$

Neglecting mean vertical motions, Eqs. (20) and (16) for $Q=0$ then reduce to a version of the model of Tennekes (1973). The value of m depends on the free flow stratification through the ratio δ/h^-, where nonzero δ is now maintained by turbulent transport of turbulence energy presumably due primarily to penetrative convection. As the stratification and $\Delta\theta$ decrease, δ is expected to increase, which reduces m. Of course, in the limit where the free flow stratification vanishes, δ and h^- are undefined. For $\delta=0$, m is roughly the fraction of the buoyancy generated turbulence energy available for mixing (conversion to potential energy) at the mixed layer top. Choosing $C_\epsilon=0.4$ for the case of a deep convectively mixed layer as discussed previously and noting that $C_0\rightarrow 0$, as the surface layer thickness becomes small with respect to h^-, we obtain $m\approx 0.2$. This value of m is within the range of various previous estimates (Tennekes, 1975). As pointed out to us by D. K. Lilly (personal communication) and noted in Tennekes (1975), this is not an independent estimate of m. If feasible, an independent but simple parameterization of dissipation is a desirable future development.

Tennekes (1973) demonstrates that for constant free flow stratification, zero mean vertical motion, and $m=0.2$, the inversion layer described by such a system of equations quickly forgets its initial conditions. Once initial conditions are forgotten, we can derive the following relationships for mixed layer depth for arbitrary m from the potential temperature jump equation (16)

for $Q=0$ and the turbulence energy equation (20):

$$\left.\begin{aligned} h(t) &\approx \left[2(2m+1)\gamma^{-1}\int_0^t (\overline{w'\theta'})_0 dt\right]^{\frac{1}{2}} \\ \Delta\theta &\approx \frac{\gamma h}{2+m^{-1}} \end{aligned}\right\}. \quad (25)$$

The mixed layer depth increases according to the square roots of time, average surface heat flux, and the inverse of the free flow lapse rate, respectively. The mixed layer depth is not particularly sensitive to m. For example, as m increases from 0.15 to 0.25, an expected typical range of m, the mixed layer depth is changed by only 7%.

We now examine the initial period where initial conditions are important. Multiplying the potential temperature jump equation (16) by h, rearranging and integrating, we obtain

$$(\Delta\theta)h^- = \tfrac{1}{2}\gamma(h^-)^2 + [(\Delta\theta)_0(h^-)_0 - \tfrac{1}{2}\gamma(h_0^-)^2] - \int_0^t (\overline{w'\theta'})_0 dt, \quad (26)$$

where the subscript 0 on $\Delta\theta$ and h^- indicates initial conditions. Combining (26) and the turbulence energy equation (20), we obtain

$$(1+\delta/h^-)\left\{\tfrac{1}{2}\gamma(h^-)^2 + (\Delta\theta)_0(h^-)_0 - \tfrac{1}{2}\gamma(h^-)_0^2 - \int_0^t (\overline{w'\theta'})_0 dt - (\Delta u^2+\Delta v^2)\theta_0/g\right\}\frac{dh^-}{dt} = [1+2C_0-2C_\epsilon(1+\delta/2h^-)](h^-)(\overline{w'\theta'})_0. \quad (27)$$

We postpone examination of effects due to shear generation and nonzero δ until later sections. Assuming constant surface heat flux, (27) simplifies to

$$[\tfrac{1}{2}h^2\gamma + (\Delta\theta)_0 h_0 - \tfrac{1}{2}\gamma h_0^2 - (\overline{w'\theta'})_0 t]\frac{dh}{dt} = mh(\overline{w'\theta'})_0. \quad (28)$$

Since h is a continuous function of time, this equation can be solved by inverting the dependent and independent variables and solving for $t=f(h)$. After inverting and rearranging, we obtain

$$\frac{-t}{h_0^2} + \gamma[2(2m+1)(\overline{w'\theta'})_0]^{-1}\left[\left(\frac{h}{h_0}\right)^2 - \left(\frac{h}{h_0}\right)^{-1/m}\right] + \frac{\left(\frac{(\Delta\theta)_0}{h_0} - \frac{\gamma}{2}\right)}{(\overline{w'\theta'})_0}\left[1-\left(\frac{h}{h_0}\right)^{-1/m}\right] = 0. \quad (29)$$

Algebraic solutions of (29) can be obtained or simply approximated for certain values of m. For example, for $m=\frac{1}{4}$,

$$h^6 - 3h^4\frac{(\overline{w'\theta'})_0}{\gamma}\left[t - \frac{(\Delta\theta)_0 h_0 - \frac{1}{2}\gamma h_0^2}{(\overline{w'\theta'})_0}\right] - h_0^6\left[1+3\frac{[(\Delta\theta)_0/h_0 - \gamma/2]}{\gamma}\right] = 0, \quad (30)$$

which reduces to a cubic polynomial. Similarly, for $m=\frac{1}{6}$,

$$h^8 - \frac{8}{3}\frac{h^6(\overline{w'\theta'})_0}{\gamma}\left[t - \frac{(\Delta\theta)_0 h_0 - \gamma h_0^2/2}{(\overline{w'\theta'})_0}\right] + h_0^8\left[1 - \frac{8}{3}\frac{[(\Delta\theta)_0/h_0 - \gamma/2]}{\gamma}\right] = 0, \quad (31)$$

which reduces to a quartic polynomial. These values represent typical estimates of m. The complete solutions for (30) and (31) are rather complicated, so we present here several limiting cases to illustrate the asymptotic character of these solutions.

For sufficiently large time, the solution (29) approaches the square-root law of Tennekes, given by Eq. (25). We examine the adjustment to this state by considering the value $m=\frac{1}{4}$. The solution to the cubic polynomial (30) becomes particularly simple for two special values of the initial potential temperature jump:

$$\left.\begin{aligned} h^2 &= h_0^2 + 3t(\overline{w'\theta'})_0/\gamma; & (\Delta\theta)_0 &= \gamma h_0/6 \\ h^2 &= h_0^2 + t(\overline{w'\theta'})_0/\gamma + O(t/h_0^2)^2; & (\Delta\theta)_0 &= \gamma h_0/2 \end{aligned}\right\}, \quad (32)$$

where the second solution is obtained by using a binomial expansion in t/h_0^2.

The mixed layer "forgets" its initial conditions when

$$\left.\begin{aligned} t &\gg \frac{h_0^2\gamma}{3(\overline{w'\theta'})_0}; & (\Delta\theta)_0 &= \gamma h_0/6 \\ t &\gg \frac{h_0^2\gamma}{(\overline{w'\theta'})_0}; & (\Delta\theta)_0 &= \gamma h_0/2 \end{aligned}\right\}.$$

Dimensionally speaking, for $(\overline{w'\theta'})_0 = 0.15$ m s^{-1} K, $\gamma = 5\times10^{-3}$ K m^{-1} and $h_0 = 200$ m, t must be much greater than 7 min and 31 min, respectively, for the above two cases.[2] Thus, when the initial depth is not larger than a few hundred meters and the initial inversion strength is within a few factors of that predicted by (25), initial conditions are important on a

[2] These time scales describe the adjustment to a state where h behaves like the square-root law (25) in time where $h=h_0$ at $t=0$. However, for the first initial condition, h already obeys a square-root law in terms of t' where $h=0$ at $t'=0$.

time scale which is small compared to the time scale for which the model is valid.

Tennekes' (1973) Eq. (28), which describes the relationship between mixed layer depth and inversion strength where initial conditions may be important, can be written for arbitrary m as

$$\Delta\theta h^{(1+1/m)} = \Delta\theta_0 h_0^{(1+1/m)} + \frac{\gamma}{(2+1/m)}[h^{(2+1/m)} - h_0^{(2+1/m)}]. \quad (33)$$

As m decreases, the exponent of h increases and, consequently, the initial conditions become unimportant more quickly in time.

Numerical iterations of the more complete equations [(14)–(16), (18), (20)] also indicate that initial conditions generally become unimportant within an hour.

5. Shear generation

The relative importance of shear generation can be represented by the ratio of shear generation to buoyancy destruction as they appear in the denominator of the mixed layer growth equation (20). This ratio is

$$\frac{[(\Delta u)^2+(\Delta v)^2]\theta_0/(gh^-)}{\Delta\theta} = \frac{\delta}{h^- \mathrm{R_b}}.$$

Estimation of this ratio from the morning mixed layer observations reported by Hall *et al.* (1975) gives an average value of 0.35. Estimation of this ratio for the data in Fig. 2 gives a value of 0.31. In deeper afternoon mixed layers shear generation at the inversion is expected to be less important. Niiler (1975) demonstrates that shear generation at the bottom of a stress-driven oceanic mixed layer is important only during an initial growth period.

The importance of shear generation can also be estimated by considering the specific contributions to shear across the inversion. Such contributions include frictional effects, baroclinicity and accelerations. Accelerations due to inertial oscillations in the mixed layer may be initiated, for example, by changes in boundary layer depth or stratification. Blackadar (1957) suggests that such accelerations may lead to development of a low-level jet. Deardorff (1973) demonstrates that when the growing morning mixed layer engulfs such a jet, large shears may develop at the mixed layer top.

Analyses by Ching and Businger (1968) and Mahrt (1974), which neglect pressure adjustments, indicate that boundary layer inertial oscillations decay according to a time scale which is comparable to or larger than the inertial period. In other words, the adjustment of the wind field to the changing mixed layer depth and stress profiles is slow compared to the time scale describing the growth of the mixed layer. Because of the difficulty in defining initial conditions for the wind field and because such initial conditions may significantly influence the mixed layer wind field throughout the day, we choose not to directly integrate the mixed layer equations of motion [(14), (15)] but instead examine the influence of idealized shear generation on the mixed layer growth.

To estimate shear at the inversion due to frictional and baroclinic effects, we assume that the convective mixing is sufficient to keep momentum well mixed (in the layer in which virtual potential temperature is well mixed) in spite of baroclinicity (Arya and Wyngaard, 1975). Rotating the coordinate system so that the stress is in the x direction, the geostrophic departure equations are then

$$\left.\begin{aligned} u - \frac{1}{h^-}\int_0^{h^-} U_g dz &= -\frac{(\overline{v'w'})_{h^-}}{fh^-} \\ v - \frac{1}{h^-}\int_0^{h^-} V_g dz &= \frac{u_*^2}{fh^-} + \frac{(\overline{u'w'})_{h^-}}{fh^-} \end{aligned}\right\}, \quad (34)$$

where u_* is the surface friction velocity. Assuming constant "thermal wind shear" components U_{gT} and V_{gT}, geostrophic flow aloft and a geostrophic surface drag relationship, and neglecting effects of baroclinicity on the surface stress (examined by Arya and Wyngaard, 1975), we obtain

$$\left.\begin{aligned} u(h^+) - u(h^-) &= U_{gT}(h^-/2+\delta) + (\overline{v'w'})_{h^-}/(fh^-) \\ v(h^+) - v(h^-) &= V_{gT}(h^-/2+\delta) - C_g^2|V_{g0}|^2/(fh^-) \\ &\quad - (\overline{u'w'})_{h^-}/(fh^-) \end{aligned}\right\}, \quad (35)$$

where C_g is the geostrophic drag coefficient and $|V_{g0}|$ the surface geostrophic wind speed. To simply indicate the possible importance of shear generation at the inversion, we neglect boundary stresses in (35) as well as acceleration contributions to the shear. For $\delta \ll h^-$, the estimate of shear at the top of the well mixed layer is

$$[(\Delta u^2)+(\Delta v)^2] \approx (U_{gT}^2 + V_{gT}^2)(h^-)^2/4. \quad (36)$$

Substituting the above estimate of shear at the inversion (36) into the mixed layer growth equation (27), and for the moment assuming $\delta \ll h$, we obtain for the case of constant surface heat flux

$$[\tfrac{1}{2}(1-S)\gamma h^2 + (\Delta\theta)_0 h_0 - \tfrac{1}{2}\gamma h_0^2 - (\overline{w'\theta'})_0 t]\frac{dh}{dt} \approx mh(\overline{w'\theta'})_0, \quad (37)$$

where

$$S \equiv (U_{gT}^2 + V_{gT}^2)\theta_0/(2\gamma g).$$

Thus, shear generation of turbulence energy in the turbulent inversion layer is most important, relative to buoyancy destruction of turbulence energy, when the stratification of the free flow is small. That is, shear-generated turbulence kinetic energy entraining free flow will be converted to potential energy more

slowly with weak free flow stratification. Eq. (37) can be transformed to an equation of the same form as the equation with no shear generation [(28)] by making the following substitutions:

$$\left.\begin{aligned}(\Delta\theta h-\tfrac{1}{2}\gamma h^2)_0 &\rightarrow (\Delta\theta h-\tfrac{1}{2}\gamma h^2)_0/(1-S)\\ t &\rightarrow t/(1-S)\end{aligned}\right\}.$$

Therefore, after the inversion growth forgets its initial conditions, the mixed layer grows in the same manner as without shear except that the time scale describing the growth decreases by a factor of $(1-S)^{-1}$; that is, the mixed layer growth rate increases by a factor of $(1-S)^{-\frac{1}{2}}$ due to shear generation at the inversion.

We now estimate possible values of S using Wangara data as guidelines. Choosing a healthy but not unreasonably large Wangara thermal wind value of 5×10^{-3} s^{-1} (e.g., Venkatesh and Csanady, 1974), $\theta_0=300$ K and $\gamma=5\times10^{-3}$ K m^{-1}, we find that $S=0.075$ in which case shear generation is not very important. However, if the overlying stratification is quite weak, such as might occur when the mixed layer is not yet as deep as the previous day's mixed layer, then shear generation could be more important. For example, if $\gamma=10^{-3}$ K m^{-1}, $S\approx0.37$. In conclusion, the above simple model indicates that shear generation due to baroclinicity is important only with both substantial baroclinicity and rather weak free flow stratification. However, the above development is only an estimate of the possible importance of shear generation in that it neglects the generation of shear due to accelerations. In actual modeling situations, one could estimate the shear at the inversion from winds computed by the model. An additional complication arises when the convectively mixed layer grows rapidly. Under such conditions, momentum may not be well mixed.

6. Comparison with Wangara Day 33

Care must be taken when comparing theoretical results with rawinsonde data since the latter represent instantaneous measurements of a fluctuating environment. Nevertheless, we will venture comparisons of model predictions with Wangara Day 33 (Clarke *et al.*, 1971) for purposes of illustrating some fundamental characteristics of mixed layer growth. Because of the difficulties in estimating shear across a relatively thin layer from a single instantaneous sounding, we choose not to model shear generation effects for this comparison. In passing, we note that shear generation as evaluated from (36) using thermal winds from Clarke *et al.*, (1971) and shear generation estimates from the actual wind measurements indicate that the mixed layer growth could be substantially increased by shear on several of the Wangara days. Day 33 is not one of these days.

Wangara Day 33 has previously been investigated by Deardorff (1974a,b) and Wyngaard and Coté, (1975) and others. On this day, skies were clear and horizontal advections appear to be small. For the numerical iterations of the modeled equations [(14)–(16), (18), (20)], we choose $C_\epsilon=0.4$ and $C_0=0$ (thus $m=0.2$). We estimate the surface heat flux for Day 33 from numerical simulations of Deardorff (1974a) and the rest of the external parameters from Clarke *et al.*, (1971) as follows:

$$\theta_0=283\text{ K}$$

$$(\overline{w'\theta'})_0=[0.19-0.05(1-t/3)]\text{ m s}^{-1}\text{ K};\quad 0\leqslant t\leqslant 3\text{ h}$$

$$(\overline{w'\theta'})_0=0.19\text{ m s}^{-1}\text{ K};\quad 3\text{ h}<t\leqslant 6\text{ h}$$

$$\gamma=28\times10^{-3}\text{ K m}^{-1};\quad h<200\text{ m}$$

$$\gamma=7.5\times10^{-3}\text{ K m}^{-1};\quad 200\text{ m}\leqslant h<300\text{ m}$$

$$\gamma=0.25\times10^{-3}\text{ K m}^{-1};\quad 300\text{ m}\leqslant h<800\text{ m}$$

$$\gamma=7.5\times10^{-3}\text{ K m}^{-1};\quad h\geqslant 800\text{ m}$$

$$(\overline{w'q'})_0=2.2\times10^{-5}\text{ m s}^{-1}$$

$$\gamma_q=1.9\times10^{-6}\text{ m}^{-1}$$

$$h_0=120\text{ m}$$

$$(\Delta\theta)_0=\frac{h_0\gamma_0}{2+1/m}\approx0.48\text{ K}.$$

Here t is expressed in hours after the initial time 0900 L.

Fig. 3 indicates that at first the modeled mixed layer grows slowly as it entrains the remainder of the stable layer generated by nocturnal surface radiational cooling. Then the mixed layer grows very quickly as it engulfs a very weakly stratified layer probably remaining from the mixed layer of the previous day. For the remainder of the day, the modeled mixed layer grows rather slowly, but as in the case of Deardorff (1974a), the predicted growth rate is roughly 50% greater than observed (Fig. 3). As is evident from numerical simulations (not shown) or by the differential square-root law (24), the afternoon growth rate is not very sensitive to likely errors in m or surface heat flux. For example, a 20% change in m or the surface heat flux would result in only $\sim$10% change in the afternoon growth rate which is small compared to the discrepancies in Fig. 3. Numerical iterations indicate that a subsidence of nearly 0.04 m s^{-1} is required to reduce the modeled growth rate to the observed growth rate. Clarke *et al.*, (1971) report instantaneous subsidence values of 0.01–0.02 m s^{-1}. Possible explanations of the above discrepancy could be attributed to various model assumptions including the neglect of advections of temperature and mixed layer depth, or to difficulties of determining mixed layer depths and small vertical motions from instantaneous soundings. Waves or other horizontal irregularities on the inversion have been observed to

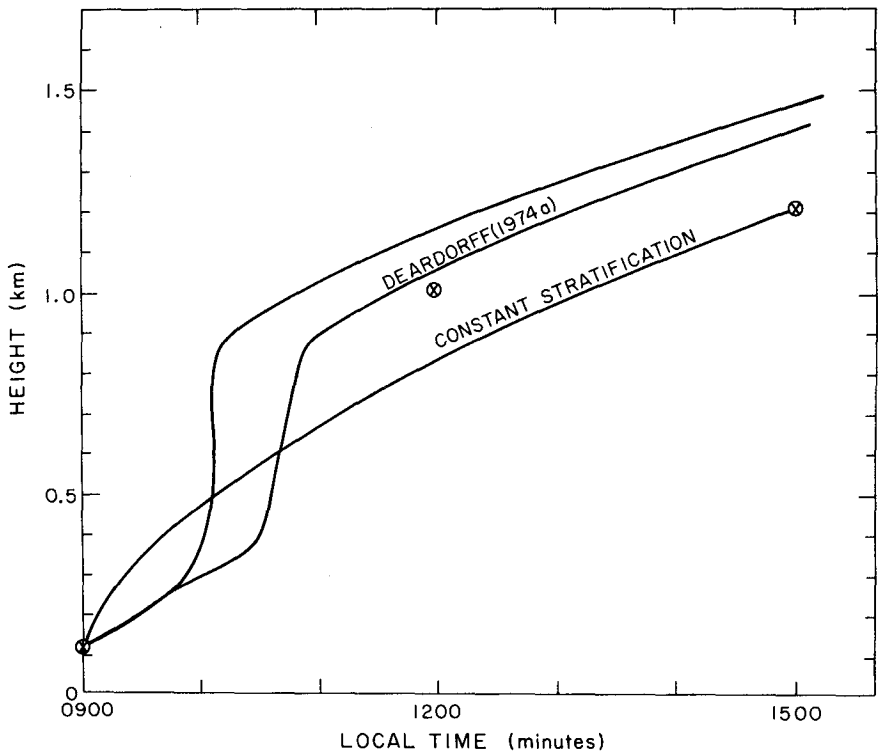

FIG. 3. Evolution of the mixed layer depth for Wangara Day 33 for the standard case discussed in text, the case of constant stratification with $\gamma = 7.5 \times 10^{-3}$ K m^{-1}, and Deardorff's (1974a) simulation. The ⊗'s at 0900, 1200 and 1500 are estimates of the observed mixed layer depth (Deardorff, 1974a).

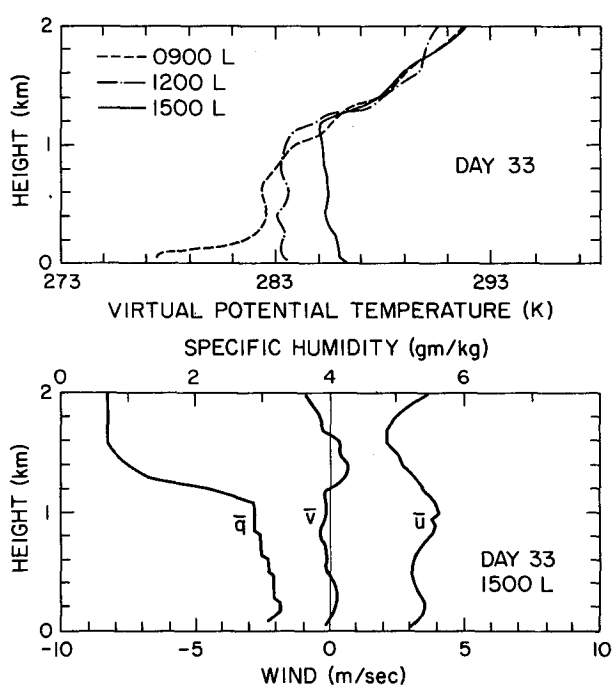

FIG. 4. Observed profiles of virtual potential temperature for Wangara Day 33 (top) and wind and specific humidity profiles for the same day at 1500 local time (bottom).

produce temporary fluctuations of inversion height of ~100 m (Rayment and Readings, 1974).

Fig. 3 also indicates that neglect of height variations of the free flow stratification results in substantial errors, particularly during the morning evolution of the mixed layer depth. Neglect of time variations of surface heat flux (not shown) causes much smaller errors.

The model predicts the specific humidity jump to be roughly 1.5×10^{-3} by afternoon when the specific humidity in the mixed layer has decreased from its morning value of 3.7×10^{-3} to about 3.0×10^{-3}. Such results compare favorably with observed values (Fig. 4). However, on the afternoon of Day 33, the specific humidity appears to be well mixed to only about 1 km whereas the modeled specific humidity is by assumption well mixed up to the predicted mixed layer depth which was several hundred meters higher.

7. Further discussion

The above results indicate that Tennekes' model reasonably predicts growth of the heated mixed layer when height variation of the free flow stratification is included. However, it appears useful to include shear generation at the inversion in significantly baroclinic

cases where the mixed layer is shallow or the free flow is only weakly stratified.

Several restrictions in the above model of the convectively mixed layer seem to particularly warrant further examination. First, specific humidity may often not be well-mixed under conditions of rapid entrainment of dry free flow or substantial mass exchange with overlying convective clouds. Second, when baroclinicity is important, horizontal advection is also likely to be important. Third, accelerations may often increase the shear and shear generation of turbulence at the inversion. Finally, an estimation of dissipation independent of free convection similarity theory seems useful as well as inclusion of nonstationarity in the turbulent inversion layer.

Extension to include the heated boundary layer where the flow is not well mixed or free convection theory is not valid is a more formidable problem, since description of the turbulence energy budget would likely involve both the surface friction and convective velocity scales. Inclusion of moist convection at the boundary layer top presents similar difficulties since transports in moist convection are organized on different scales governed by an additional external parameter involving latent heat release.

Acknowledgments. We gratefully acknowledge Dr. Ernest Peterson who suggested the flow problem to us, Dr. James Deardorff for his helpful suggestions and plots of the Wangara data, and Dr. Harumi Isaka who analyzed the aircraft data presented in Fig. 2. This research was partially supported by Grant GA-37571, Atmospheric Sciences Section, National Science Foundation.

REFERENCES

Arya, S. P. S., and J. C. Wyngaard, 1975: Effect of baroclinicity on wind profiles and the geostrophic drag law for the convective planetary boundary layer. *J. Atmos. Sci.*, **32**, 767–778.

Atlas, D., J. I. Metcalf, J. H. Richter and E. E. Gossard, 1970: The birth of "CAT" and microscale turbulence. *J. Atmos. Sci.*, **27**, 903–13.

Blackadar, A. K., 1957: Boundary layer wind maxima and their significance for the growth of nocturnal inversions. *Bull. Amer. Meteor. Soc.*, **38**, 283–290.

Browning, K. A., J. R. Starr and A. J. Whyman, 1973: The structure of an inversion above a convective boundary layer as observed using high-power pulsed Doppler radar. *Bound.-Layer Meteor.*, **4**, 91–112.

Carson, D. J., 1973: The development of a dry inversion-capped convectively unstable boundary layer. *Quart. J. Roy. Meteor. Soc.*, **99**, 450–467.

Ching, Jason K. S., and J. A. Businger, 1968: The response of the planetary boundary layer to time varying pressure gradient force. *J. Atmos. Sci.*, **25**, 1021–1025.

Clarke, R. H., A. J. Dyer, R. R. Brook, D. G. Reid and A. J. Troup, 1971: The Wangara experiment: Boundary layer data. Tech. Paper No. 19, Div. Meteor. Phys., CSIRO, Aspendale, Australia, 340 pp.

Csanady, G. T., 1974: Equilibrium theory of the planetary boundary layer with an inversion lid. *Bound.-Layer Meteor.*, **6**, 63–80.

Deardorff, J. W., 1969: Numerical study of heat transport by internal gravity waves above a growing unstable layer. *Phys. Fluids*, **12**, Suppl. II, 184–194.

——, 1973: An explanation of anomalously large Reynolds stresses within the convective planetary boundary layer. *J. Atmos. Sci.*, **30**, 1070–1076.

——, 1974a: Three-dimensional numerical study of the height and mean structure of a heated planetary boundary layer. *Bound.-Layer Meteor.*, **7**, 81–106.

——, 1974b: Three-dimensional numerical study of turbulence in an entraining mixed layer. *Bound.-Layer Meteor.*, **7**, 199–266.

Denman, K. L., 1973: A time-dependent model of the upper ocean. *J. Phys. Oceanogr.*, **3**, 173–184.

Hall, F. F., J. D. Edinger and W. D. Neff, 1975: Convective plumes in the planetary boundary layer, investigated with an acoustic echo sounder. *J. Appl. Meteor.*, **14**, 513–523.

Holloway, J. L., 1958: Smoothing and filtering of time series and space fields. *Advances in Geophysics*, Vol. 4, Academic Press, 351–389.

Kerman, B. R., 1974: An energy budget for waves and turbulence within an inversion. *Bound.-Layer Meteor.*, **6**, 443–458.

Kraus, E. B., and J. S. Turner, 1967: A one-dimensional model of the seasonal thermocline, Part II. *Tellus*, **19**, 98–105.

Lenschow, D. H., 1974: Model of the height variation of the turbulence kinetic energy budget in the unstable planetary boundary layer. *J. Atmos. Sci.*, **31**, 465–474.

Lilly, D. K., 1968: Models of cloud-topped mixed layers under a strong inversion. *Quart. J. Roy. Meteor. Soc.*, **94**, 292–309.

Mahrt, L., 1974: Time-dependent, integrated, planetary boundary layer flow. *J. Atmos. Sci.*, **31**, 457–464.

Metcalf, J. I., and D. Atlas, 1973: Microscale ordered motions and atmospheric structure associated with thin echo layers in stably stratified zones. *Bound.-Layer Meteor.*, **4**, 7–35.

Niiler, Peter, 1975: Deepening of the wind-mixed layer. *J. Marine Res.* (in press).

Pennell, W. T., and M. A. LeMone, 1974: An experimental study of turbulence structure in the fair-weather trade wind boundary layer. *J. Atmos. Sci.*, **31**, 1308–1323.

Pollard, R. T., P. B. Rhines and R. O. R. Y. Thompson, 1973: The deepening of the wind-mixed layer. *J. Geophys. Fluid Mech.*, **3**, 381–404.

Rayment, R., and C. J. Readings, 1974: A case study of the structure and energetics of an inversion. *Quart. J. Roy. Meteor. Soc.*, **100**, 221–233.

Readings, C. J., E. Golton and K. A. Browning, 1973: Fine-scale structure and mixing within an inversion. *Bound.-Layer Meteor.*, **4**, 275–287.

Stull, R. B., 1973: Inversion rise model based on penetrative convection. *J. Atmos. Sci.*, **30**, 1092–1099.

Tennekes, H., 1973: A model for the dynamics of the inversion above a convective boundary layer. *J. Atmos. Sci.*, **30**, 558–567.

——, 1975: Reply (to S. S. Zilitinkevich). *J. Atmos. Sci.*, **32**, 992–995.

Thompson, R. O. R. Y., 1973: Stratified Ekman boundary layer models. *Geophys. Fluid Dyn.*, **5**, 201–210.

Venkatesh, S., and G. T. Csanady, 1974: A baroclinic planetary boundary-layer model, and its applications to the Wangara data. *Bound.-Layer Meteor.*, **5**, 459–473.

Willis, G. E., and J. W. Deardorff, 1974: A laboratory model of the unstable planetary boundary layer. *J. Atmos. Sci.*, **31**, 1297–1307.

Wyngaard, J. C., and O. R. Coté, 1971: The budgets of turbulent kinetic energy and temperature variance in the atmospheric surface layer. *J. Atmos. Sci.*, **28**, 190–201.

——, and O. R. Coté, 1975: The evolution of the convective planetary boundary layer—A higher-order-closure model study. *Bound.-Layer Meteor.*, **7**, 289–308.

Zilitinkevich, S. S., 1975: Comments on "A model for the dynamics of the inversion above a convective boundary layer." *J. Atmos. Sci.*, **32**, 991–992.